Interleukin-22 regulates interferon lambda expression in a mice model of pseudomonas aeruginosa pneumonia

Alexis Broquet, Anissa Besbes, Jérôme Martin, Cédric Jacqueline, Mickael Vourc'h, Antoine Roquilly, Jocelyne Caillon, Régis Josien, Karim Asehnoune

Interleukin-22 regulates interferon lambda expression in a mice model of *Pseudomonas aeruginosa* pneumonia

Alexis Broquet[a]*, Anissa Besbes[a]*, Jérôme Martin[c,d,e], Cédric Jacqueline[a], Mickaël Vourc'h[a,b], Antoine Roquilly[a,b], Jocelyne Caillon[a], Régis Josien[c,d,e], Karim Asehnoune [a,b,#]

Affiliations

(a) Laboratoire UPRES EA3826 « Thérapeutiques cliniques et expérimentales des infections », IRS2 – Nantes Biotech, Université de Nantes, Nantes, France

(b) CHU Nantes, Pôle anesthésie réanimations, Service d'anesthésie réanimation chirurgicale, Hôtel Dieu, Nantes, F-44093, France

(c) Centre de Recherche en Transplantation et Immunologie UMR1064, INSERM, Université de Nantes, Nantes, France

(d) Institut de Transplantation Urologie Néphrologie (ITUN), CHU Nantes, Nantes, France

(e) Laboratoire d'Immunologie, CHU Nantes, Nantes, France

Correspondent footnote :

#: corresponding author: Karim Asehnoune, MD, PhD. Laboratoire EA3826. IRS2 – Nantes Biotech. 22 Bd Benoni Goullin 44200 Nantes, France. karim.asehnoune@chu-nantes.fr - +33 (0)2 40 08 30 05.

Footnote page :

Conflict of interest: none to declare

*: Both authors contributed equally.

Funding statement: This work was supported only by institutional funds.

Author contributions:

Conceived and designed the experiments: AB, AB and KA. Performed the experiments: AB, AB, CJ, MV. Analysed the data: AB, AB and KA. Contributed reagents/materials/analysis tools: JM, JC RJ. Wrote the paper: AB, AB. Edited the paper: JM, CJ, MV, JC, AR, RJ and KA Statistical analysis: AB.

Running title: IFN-λ improves pneumonia outcome

Abbreviations: AMP: antimicrobial peptides; CFU: colony forming units; IL-1β: interleukin 1β; IFN-λ: interferon lambda; IL-8; interleukin 8; IL-22: interleukin 22; moi: multiplicity of infection; PA: *Pseudomonas aeruginosa*; SIOX: Single Integrative Object eXtraction.

Key words: alveolar epithelial cells, interleukin-22, interferon-λ, Pseudomonas aeruginosa, host response, neutrophils

Main text count: 3245

1. Introduction:

Pseudomonas aeruginosa (PA) is one of the leading cause of nosocomial pneumonia in immunosuppressed and ICU patients (Kollef et al., 2014) ; PA is also the main cause of chronic respiratory infection in Cystic fibrosis patients (Lyczak et al., 2002). Due to increasing resistance to antibiotics with emergence of multidrug resistant bacteria strains, it is imperious to find out an alternative to antibiotics to treat bacterial infections.

Alveolar epithelial cells are the key players in the defense against pathogens (Fehrenbach, 2001) (Leiva-Juárez et al., 2017). Not only epithelial cells constitute a physical barrier against bacteria, but they also sense pathogens via their Pathogens Recognizing Receptors and secrete chemokines, cytokines and anti-microbial peptides (AMPs) to initiate immune response (Thorley et al., 2011).

Interleukin (IL-) 22 belongs to the IL-10 family and acts primarily on epithelial cells as they are the only cell type to express the IL-22R subunit IL-22RA1 (Wolk et al., 2002). IL-22 restricted action on epithelial cells places this cytokine at the bridge between the immune system and epithelial surfaces (Witte et al., 2010; Zenewicz and Flavell, 2011). IL-22 action is dependent of the host inflammatory status as it may be either deleterious, i.e. in psoriasis (Martin et al., 2017; Sabat et al., 2013; Zheng et al., 2007), or beneficial against pathogens (Eidenschenk et al., 2014). In the lungs, IL-22 was originally described to enhance the production of antimicrobial peptides (AMPs) such as β-defensin 2 (BD2) (Wolk et al., 2006) and had been shown to be protective against *S. pneumonia* (Trevejo-Nunez et al., 2016), and *K. pneumonia* (Aujla et al., 2008) infection. Interestingly, PA actively impaired IL-22-mediated mucosal defense (Guillon et al., 2016) and we previously showed a transient increase of IL-22 and demonstrated a beneficial role of this cytokine during a PA acute pneumonia model in mice as IL-22 levels are negatively correlated to lung damages (Broquet et al., 2017).

Type-III interferons, also named IFN-λ 1-4 in humans or IL-28/IL-29 in mice, are cytokines belonging to the same IL-10 cytokine family than IL-22. In respiratory tract, human myeloid and epithelial cells produce IFNλ upon stimulation (Lazear et al., 2015). IFN-λ members and IL-22 share the same IL-

10Rβ chain of their heterodimeric receptor (Sheppard et al., 2003). Protective functions of IFN-λ members have extensively been documented during antiviral host response (Andreakos et al., 2018; Lazear et al., 2015) and the role of this cytokine family emerged during bacterial infection (Syedbasha and Egli, 2017). Recent works highlighted the role of IFN-λ during bacterial infection in epithelial defense by promoting epithelial integrity, preventing bacterial spread (Odendall et al., 2017) and reducing neutrophil accumulation (Galani et al., 2017). In the context of PA pneumonia, Cohen et al. previously showed an IFN-λ induction in the broncho-alveolar fluid of infected mice (Cohen and Prince, 2013a). In the present work, we hypothesized that IL-22 may regulate IFN-λ expression during *P. aeruginosa* pneumonia. ~~exert its protective effects trough induction of IFN-λ~~. We first showed, *in vitro,* that IL-22 stimulation of epithelial cells infected with PA enhanced IFN-λ expression. We also observed, *in* vivo, that IL-22 administration or neutralization is associated with an increase or a decrease of IFN-λ during pneumonia. We finally addressed the beneficial role of IFN-λ *in vivo*. IFN-λ2 administration resulted in a significant improvement of mouse clinical score and lung histology associated with a dampening of the neutrophil recruitment at the site of infection, highlighting the beneficial roles of IL-22 and IFN-λ during bacterial pneumonia ~~and their synergistic action~~.

2. Materials and Methods:

2.1. Bacterial strains, cell line and mice

P. aeruginosa (PA) PAO1 and PAO1-GFP were grown in Brain Heart Infusion broth overnight at 37°C under agitation. Immediately before use, the bacterial pellet was washed twice with PBS and the inoculum was calibrated by nephelometry at 10^9 colony-forming unit (CFU)/mL. Human alveolar epithelial cell line A549 (mycoplasma free) were obtained from Dr Vié (Nantes, France) and maintained in RPMI 1640 (ThermoFisher Scientific) complemented with 10% heat-inactivated fetal bovine serum, Penicillin (100 U/mL), Streptomycin (100µg/mL) and 1% L-Glutamine. Cells were maintained at 37°C under a humidified atmosphere of 5% CO2 in air. Depending on experiments, cells were seeded in culture 12 wells or 24 wells plate at a density of 10^6 cells/mL and 5.10^5 cells/mL respectively. Eight-to-ten-week-old pathogen-free female RjOrl:SWISS mice (weight, 29–32 g) were purchased from Janvier Laboratories (Le Genest Saint Isle, France). Mice were maintained on a 12-hour light/dark cycle with access to food and water ad libitum. The animals were treated in accordance with institutional policies and the guidelines stipulated by the animal welfare committee. Experimental procedures were approved by the Animal Ethics Committee of the Pays de le Loire (APAFIS authorization #9124-2017022317236247-v2).

2.2. Cells treatment and Infection

Cells were starved overnight before infection. All infections were performed in antibiotic-free medium at a multiplicity of infection (MOI) 1:1 or 10:1 (bacteria load). Cells were stimulated with human recombinant IL-22 at 100 ng/mL (Miltenyi Biotec, Paris, France). Cells were infected during 2h with IL-22 co-treatment then supernatant was removed and replaced by new media containing 200µg/mL of gentamicin until 24h post-infection.

2.3. Bacterial load

For bacterial load assessment, serial dilutions of supernatants were performed and incubated at 37°C. After 24 h of incubation, viable counts were expressed as the mean±SD $\log_{10}$ CFU/mL.

2.4. Cells lysis and Immunoblotting

Cells were washed twice with cold PBS then lysed in RIPA buffer (Cell Signaling Technology, The Netherland), with phosphatase and Protease inhibitors cocktails (Sigma, St Quentin Fallavier). Proteins were quantified with BCA protein assay kit (ThermoFisher Scientific) and separated in SDS-acrylamide gel (40 µg per lane, 10% TGX Precast Gel, Bio-Rad), and transferred to nitrocellulose membrane before 1 hour saturation at room temperature under agitation in TBS, BSA 5%, 0.1% Tween 20 (Sigma, St Quentin Fallavier, France). Membranes were incubated with primary rabbit anti-phospho-STAT-3 or STAT3 antibody (Ab) (1:1000, Cell Signaling Technology). Membranes were then incubated with secondary anti-rabbit HRP antibody (1:1000 Cell Signaling) for 1h at RT and with the SuperSignal West Pico PLUS kit for 5 min (ThermoFisher Scientific). Immunoreactives bands were visualized with the Azure c500 instrument (Azure Biosystems).

2.5. STAT3 phosphorylation in A549 by flow cytometry

STAT3 phosphorylation was assessed using BD Phosflow kit according to manufacturer's instructions (BD Bioscience) using an alexaFluor488-conjugated anti-phospho-STAT3 antibody. Data acquisition was realized on viable single cells using an Accuri C2 cytometer (BD Bioscience).

2.6. Human cytokines quantification by Enzyme-Linked ImmunoSorbent Assay (ELISA)

All human ELISA kits were from ThermoFisher Scientific unless otherwise indicated. Harvested supernatants were centrifuged 20 min at 4°C at 12000g and stored at -80°C before, IL-8, IL-22, IFN-λ2 quantification by ELISA according to the manufacturer's instructions.

2.7. RNA extraction and Reverse Transcriptase Polymerase Chain Reaction (RT-PCR)

2h post-infection cells were washed twice with cold PBS then harvested and total RNA was extracted with High Pure RNA Tissue Kit (Roche Diagnostic) according to manufacturer's recommendations. 1µg of RNA was used for Reverse Transcription in cDNA using Transcriptase III kit (Invitrogen, Villebon Sur Yvette, France). Quantitative real time PCR was performed with Maxima SYBR Green/ROX qPCR kit (ThermoFisher Scientific). Relative mRNA expression levels were quantified

using the $2^{-\Delta\Delta Ct}$ method with normalization to actin gene expression. Primer sequences (Sigma) are listed in supplemental digital content table 1.

2.8. Confocal Microscopy

A549 cells were seeded in Lab-Tek chambers (ThermoFisher Scientific) at a density of 5.10^5cells/mL/well and infected with PAO1-GFP strain. Following 4h of infection, cells were washed twice with cold DPBS, fixed 10 min with PFA 4% (Sigma) and permeabilized with 0.1% Triton X100 (Sigma) for 10 min. Cells were stained with a mouse anti-IL-22RA (ThermoFisher Scientific) primary antibody overnight at 4°C following AlexaFluor 647 conjugated anti-mouse secondary antibody (ThermoFisher Scientific). β-actin and nuclei were respectively stained with AlexaFluor 568 phalloïdin (ThermoFisher Scientific) 30 min at room temperature and DAPI (ThermoFisher Scientific) 10 min. Prolong fade (ThermoFisher Scientific) mounted slides were monitored by confocal microscopy (Carl Zeiss, Oberkochen, Germany). Captured images were analyzed with Fiji software.

2.9. Murine AEC flow cytometry

Lungs were removed and digested 45' at 37°C in RMPI-BSA 0,1% containing 0,7% type-3 collagenase (Worthington, Freehold, USA) and 0,1% DNase I (Sigma Aldrich). After red blood cell lysis (BioLegend), cells were incubated 40' with the following antibodies: CD45-FITC (clone 30-F11. BD Bioscience), CD31-brilliant violet 605 (clone 390. BD Bioscience), T1-α-APC (clone 8.1.1. BioLegend) and Ep-Cam (CD326)-PeCy7 (clone G8.8. BioLegend), IL-22RA1-PE (clone 496514, Bio-Techne) and rat IgG2a,k-PE isotype control (clone eBR2a . ThermoFisher Scientific). Samples were acquired on LSR-II (BD Bioscience) and analyzed using Flowjo Software (TreeStar Inc). Single lived cells were gated as $CD45^{neg}$ $CD31^{neg}$ $Ep\text{-}Cam^{pos}$ $T1\text{-}\alpha^{pos}$ type-I AECs (ATI), $CD45^{neg}$ $CD31^{neg}$ $Ep\text{-}Cam^{pos}$ $T1\text{-}\alpha^{neg}$ type-II AECs (ATII) and $CD45^{neg}$ $CD31^{neg}$ $Ep\text{-}Cam^{neg}$ (non AECs).

2.10 Mouse pneumonia and treatment

Under anesthesia, mice were placed in dorsal recumbency and a transtracheal insertion of a 24-gauge

feeding needle was performed to inject 75µL of a bacterial suspension adjusted to 10^8 CFU/mL ($7{,}5x10^6$ CFU/mouse). 50µg of neutralizing IL-22 (Broquet et al., 2017) or IFN-λ2 (Bio-Techne) antibodies (and their respective isotype control) were i.v. administrated 16 hours before the induction of pneumonia. 1µg of rIL-22 (Miltenyi, diluted in PBS-BSA 0,1%) or rIL28A (referred in the text as IFNλ2. Biotechne, diluted in PBS-BSA 0,1%) or PBS-BSA 0,1% (vehicle control) was administrated intra-tracheally at the time infection and 8 hours post infection. Mouse body weight was evaluated daily and lungs were collected at 24 hours post infection for subsequent analysis. For histology, lungs were inflated with 1mL of 4% formalin and processed for hematoxylin / eosin and neutrophil (Ly6-G) staining as previously described. Bacteria loads and IL1β level quantification in the lung homogenates were performed as previously described (Broquet et al., 2017). For Bronchoalveolar Fluid (BALF) analysis, euthanized mice were put in dorsal recumbency and the tracheas were exposed. A 22-gauge catheter was inserted in the trachea and the lungs were washed 3 times with 1 mL of cold PBS. IFN-λ2 quantification was performed in BALF by ELISA following manufacturer's instructions (ThermoFisher Scientific).

2.11. Statistical analysis

Data were analyzed by Kruskal-Wallis test for multiple group comparisons using the GraphPad Prism software (La Jolla, CA. United States). Dunn's multiple comparison test was used as post hoc test for intergroup comparisons. $p< 0.05$ was considered statistically significant.

3. Results

3.1. Type-II AECs, not type-I AECs express IL-22RA1 in normal and PAO1-infected conditions

IL-22RA1 expression is restrained to non hematopoietic cells such as endothelial and epithelial cells. Using flow cytometry, we demonstrate, that within AECs, IL-22RA1 expression is restricted to type-II AECs (ATII) in lungs of non-infected and PAO1-infected mice (figure1a). Using a human ATII cell line in vitro (A549 cells), both uninfected and PAO1-infected cells express IL-22RA1 as shown by confocal microscopy (figure 1b) and PAO1-infection does not modify IL-22RA1 mRNA expression (figure 1c).

3.2. IL-22 signaling is functional in A549 cells during PAO1 infection

A549 cells incubation with IL-22 shows a rapid and transient STAT3 phosphorylation in uninfected A549 cells (figure 2a) similar to the observation of Whittington et al. (Whittington et al., 2004), demonstrating the functionality of the IL-22RA1 signaling pathway in this cell line. Interestingly, PA infection does not interfere with IL-22RA1 signaling as a similar STAT3 phosphorylation rate is observed in infected- compared to uninfected-cells in IL-22 condition (figure 2b).

IL-22/STAT3 pathway is known to drive the expression of antimicrobial peptides (Li et al., 2015; Moyat et al., 2017). IL-22 incubation on A549 cells during infection enhances Reg1-α and BD2 compared to infection alone (figure 2c) without decreasing bacterial load in vitro (figure 2d). We previously demonstrated that IL-22 levels are negatively correlated to IL-8 expression in A549 cells and during a mouse pneumonia model (Broquet et al., 2017). Consistent with our previous findings, IL-22 treatment during infection decreases IL-8 production during PAO1 infection at the mRNA and protein levels (figure 2e, left and right panel respectively).

3.3. IL-22 regulates IFN-λ expression by A549 cells during infection

Member of the IFN-λ family (IFN-λ1-3) have been suggested to play a role in the reinforcement of epithelial barrier during bacterial infection (Odendall et al., 2017) and IL-22 administration enhanced IFN-λ expression in intestinal viral infection (Xue et al., 2017). We, then, assess the ability of IL-22 to

increase IFN-λ expression in A549 cell line. IL-22 significantly induces all IFN-λ member mRNA expression in PAO1-infected A549 cells (figure 3a-b). IFN-λ2 increased is confirmed by ELISA in which IL-22 administration leads to detectable IFN-λ2 protein level only in PA-infected A549 cells (figure 3c). In a murine pneumonia model, IFN-λ expression increases after 3 hours with a return to baseline at 24h (figure 3d. white bars), similar to the observation of Cohen et al (Cohen and Prince, 2013a). Interestingly, in mice intratracheally treated with IL-22, the IFN-λ drop at 24 hours was no longer observed compared to PBS-treated animals suggesting that IL-22 treatment maintains high levels of IFN-λ during infection (figure 3d. Grey bars). To confirm that IL-22 may play a role on IFN-λ levels in vivo, we depleted mice on IL-22 in the lungs using a neutralizing antibody approach. We previously showed that such approach led to a significant decrease of IL-22 in the lungs (Broquet et al., 2017). Interestingly, in vivo IL-22 neutralization completely abolished IFN-λ up-regulation during PA pneumonia (figure 3e). Altogether these data strongly suggest that IL-22 may modulate IFN-λ levels in the lungs.

3.4. In vivo IFN-λ administration dampens lungs inflammation during bacterial pneumonia

To assess the IFN-λ protective functions during PA pneumonia, we evaluated the impact of IFN-λ2 treatment in mice during PAO1 pneumonia. IFN-λ2 administration significantly reduces the body weight loss (figure 4a) and improved the mouse clinical score (figure 4b), without bacterial load reduction in the lungs (figure 4c). IFN-λ2 treatment led to a decrease of the alveolar spaces shrinking during infection (figure 4e) associated with fewer infiltrated cells in the alveoli (figure 4d). To confirm that IFN-λ2 decreased cell infiltrate, we quantified neutrophil accumulation following infection. IFN-λ2 administration at the time of infection is associated with a decrease of neutrophil recruitment (figure 4f and g) and IL-1β level decrease in the lungs (figure 4h) highlighting the anti-inflammatory properties of IFN-λ2 during bacterial pneumonia. In the same manner, IFN-λ2 neutralization induced a dramatic increase of IL-1β in the lungs (figure 5a) associated with an aggravated lung damages (figure 5b). Not surprisingly, IFN-λ2 neutralization does not impaired beneficial rIL-22 treatment during pneumonia as shown by IL1-β reduction levels compared to untreated mice (figure 5a) and

230 decrease lung damages (figure 5b). This last point suggests that the beneficial action of IL-22 is not

231 restricted to IFN-λ levels in our pneumonia model.

232

4. Discussion

Our results can be summarized as follow: IL-22 increases the expression of IFN-λ by AECs upon infection in vitro. In vivo, IL-22 administration is associated with an increase of IFN-λ in the lungs whereas IL-22 neutralization abolished IFN-λ up-regulation during PA infection; these *in vivo* data suggest that IL-22 may modulate IFN-λ levels in vivo. This IL-22 effect on IFN-λ levels might be of interest as IFN-λ administration display protective functions in a mouse model of PA pneumonia (decrease of neutrophils influx and IL-1β levels).

Only few cells (non hematopoietic lineage), among them AECs, can respond to IL-22 due to IL-22RA1 restriction of expression. We demonstrate for the first time that among AECs, type-II AEC (ATII) are the only responsive cells to IL-22 stimulus in the lungs of mice. IL-22 modulates host immunity by increasing the production of AMPs and dampening host damages (neutrophil influx, IL-1β levels). The present results confirm our previous findings showing that IL-22 decreases the production of neutrophil-chemoattractant MIP-2, and this alteration was correlated with a decrease of neutrophil recruitment at the site of infection (Broquet et al., 2017).

The interferon family is composed of 3 subgroups (type I, II, and III) which signal through STAT transcriptions factors inducing the expression of over 300 IFN dependent genes (Egli et al., 2014). The type III IFN-λ receptor is abundantly expressed in the lungs and was demonstrated to be very important for host defense against virus. However, endogenous IFN-λ role during bacterial infection remain uncertain. Type III IFN was also demonstrated to kill the intracellular bacteria *Listeria monocytogenes* along with a reduction of colonization of the spleen and liver (Lebreton et al., 2011). Very few data are available concerning the role of IFN-λ in the defense of the host against extracellular bacterial infections (Cohen and Prince, 2013a). Nonetheless, the effects of IFN-λ such as maturation or differentiation of DC, upregulation of MHC I and II, production of NFκB dependent cytokines are relevant to the immune response of extracellular bacterial infections (Gallagher et al., 2010; Koltsida et al., 2011; Pekarek et al., 2007). In accordance with these data, the current results clearly show a beneficial role of intra-tracheal IFN-λ2 administration during a PA pneumonia model

along with a dampening neutrophil recruitment whereas IFN-λ2 neutralization dramatically increase IL-1β levels in mice. This is consistent with previous studies showing similar effect of IFN-λ in allergic asthma and collagen-induced arthritis models (Blazek et al., 2015; Yan et al., 2017). Similar with our findings, Blazek et al, in an arthritis model, showed anti-inflammatory effect of IFN-λ1 through reduction of the recruitment of IL-1β expressing neutrophils (Blazek et al., 2015). However, our findings are in discrepancy with the results of Cohen et al. who observed a decrease of lung inflammation following PA pneumonia in IFN-λ receptor (IFNλR) knock-out (KO) mice (Cohen and Prince, 2013b). IFN-λR KO mice had a significant higher IL-22 expression in the lungs at the baseline or following influenza infection (Planet et al., 2016) suggesting a compensatory mechanism in these animals. This could explain the contradictory results observed between wild-type in our study and IFN-λR knock-out mice during PA infection. IL-22 neutralization completely abolished the increase of INF-λ levels during infection. IL-22 levels during PA pneumonia seems critical as PA proteolytically degrades IL-22 (Guillon et al., 2016) which may lead to a decrease of IFN-λ in infected tissues. The use of exogenous IL-22, to counteract IL-22 degradation by the bacteria, led to an improvement of lung damages (Broquet et al., 2017) correlated with an increase of IFN-λ. We previously showed that IL-22 level in the lungs is inversely correlated to neutrophil accumulation during PA pneumonia (Broquet et al., 2017). According to Guillon et al, we may hypothesize that IL-22 degradation by PA led to a decrease of IFN-λ in the tissue with the consequence of an overwhelming neutrophil accumulation. We, thus, observe *in vitro* and in vivo, for the first time, the ability of IL-22 to enhance IFN-λ expression in the BALF strengthening the link between IL-22 and IFN-λ. Interestingly, Hernández et al. described a beneficial and synergistic effect of IL-22 and IFN-λ administration in a mouse rotavirus infection model. In their study, IL-22 protection was dependent on IFN-λ expression, and combined IL-22 and IFN-λ administration enhances expression of Interferon-stimulated genes (ISGs) protecting epithelial cells against viral replication (Hernández et al., 2015). In our mouse model, we hypothesized a dependency of expression of IFN-λ to IL-22 during PA infection. This is of importance as recent literature highlighted the role of IFN-λ during innate and adaptive immune responses (Ye et al., 2019). However, in our model, IFN-λ2 neutralization in vivo did not alter the

286 ability of IL-22 to minor IL-1β levels suggesting that IL-22 may alos display some protective effect in
287 an IFN-λ independent manner. Exact contribution of IFN-λ during bacterial pneumonia remains
288 unclear, as recognition of cells producing this cytokine is a matter of debate. On one hand, AEC
289 (Sommereyns et al., 2008), macrophages (Wolk et al., 2008) and neutrophils (Blazek et al., 2015) have
290 been found to be responsive to IFN-λ. On the other hand, AECs and mono-derived dendritic cells have
291 been described as a source of IFN-λ in vitro (Kotenko et al., 2003).

292 In conclusion, this study reveals new properties of IL-22 during bacterial pneumonia by its ability to
293 impact on IFN-λ during bacterial pneumonia. This result may prove important since IFN-λ2
294 demonstrate a clinical and histological beneficial role in a mouse model of PA pneumonia.

295

296 **Acknowledgements**

297 We thank the Cellular and Tissular Imaging Core Facility of Nantes University (MicroPICell)
298 for assistance in histological sample preparation and analysis. We thank the Cytometry Core
299 (CytoCell) for the technical assistance.

300

Figure legend:

Figure 1: IL-22 signaling is not altered during PAO1 infection in type-II AECs.

[a] IL-22RA1 expression on single $CD45_{neg}$ $CD31_{neg}$ lived cells in the lungs by flow cytometry. ATI: Type-I Alveolar epithelial cells gated as Ep-Cam_{pos} T1-α_{pos}. ATII: Type-II Alveolar epithelial cells gated Ep-Cam_{pos} T1-α_{neg}. Non AECs gated Ep-Cam_{neg}. Dashed line: isotype control Ab. Solid line: IL-22RA1 Ab in sham mice. Filled histogram: IL-22RA1 in infected mice. [b] Confocal microscopy of non-infected (upper panel) and 4h PAO1-infected A549 cells (lower panel). Blue: nuclei, red: β-actin, white: IL-22RA1, green: PAO1-GFP. Magnification x40. Bar = 25µm. [c] IL-22RA1 mRNA expression by real-time PCR from PAO1-infected A549 cells treated or not with IL-22. Boxes represent median (interquartile range). n.s.: not significant.

Figure 2: IL-22 incubation modulates cell response to infection

[a] Western blot of phospho-STAT3 expression from non-infected and PAO1-infected A549 cells treated or not with IL-22. [b] p-STAT3 evaluation in 15 minutes infected-A549 by flow cytometry. Dot plots: left: non infected; middle: IL-22 alone; right: IL-22 + PAO1. Right histogram: Percent of A549 expressing p-STAT3 following treatment [c] Reg1-α and β-defensin-2 mRNA expression by real-time PCR from 2h PAO1-infected A549 cells treated or not with IL22. Boxes represent median (interquartile range). [d] Bacterial load in supernatant from 24h PAO1-infected A549 cells treated or not with IL-22. Boxes represent median (interquartile range). Dashed bar: detection threshold [e] IL-8 mRNA relative expression from 2h PAO1-infected A549 cells treated or not with IL-22 (left panel) and IL-8 protein levels by ELISA from 24h PAO1-infected A549 cells treated or not with IL-22 (right panel. sensitivity limit: 2pg/mL). Boxes represent median (interquartile range). Data are representative of two independent experiments. *: $p<0.05$ **: $p<0.001$.

Figure 3: IL-22 enhanced IFN-λ expression in PAO1 infected cells

[a-b] IFN-λ1 and IFN-λ2/3 mRNA relative expression from 2h PAO1-infected A549 cells treated or not with IL-22. Boxes represent median (interquartile range). [c] IFN-λ2 protein levels from 24h PAO1-infected A549 cells treated or not with IL-22 (dashed line: sensitivity limit 15,6pg/mL). Boxes represent median (interquartile range). n.d. : not detected. Data are representatives of two independent experiments. [d] IFN-λ2 quantification by ELISA in BALF of infected mice treated or not with IL-22 (sensitivity limit: 0,3pg/mg of proteins). [e] IFN-λ2 quantification by ELISA in BALF of infected mice treated or not with neutralizing anti-IL-22 antibody. Boxes represent median (interquartile range). n=5 per group. *: $p<0.05$ **: $p<0.001$

Figure 4: In vivo IFN-λ2 administration improves mice outcome and dampens neutrophil recruitment during infection.

[a] Daily body weight evaluation of infected mice vehicle- or IFN-λ2-treated. [b] Mouse clinical score of 24h-infected mice vehicle- or IFN-λ2-treated. [c] Bacterial counts (expressed in $\log_{10}$ colony-forming units (CFU)/gram of organ) in the lungs of 24h-infected mice vehicle-treated or IFN-λ2-treated. Data are representative of two independent experiments. Dashed line: threshold limit [d – left panel] Lung histological analysis from PAO1 infected mice 24h vehicle-treated (upper panel) or IFN-λ2-treated (lower panel). Magnification x40. Bar = 25µm. [d – right panel]. [e] Alveolar space quantification by SIOX analysis of histology slides presented in d (3 mice per group. 4 fields per slide). [f] Ly6-G IHC of lung section from 24h-infected PAO1 mice vehicle-treated (upper panel) or IFN-λ2-treated (lower panel). Magnification x40. Bar = 25µm. [g] Quantification of Ly6-G positive pixels surface area by SIOX analysis of the slides presented in f. (3 mice per group. 4 fields per slide). [h] IL-1β concentration assessment by ELISA in lung homogenates of 24h infected mice vehicle-treated or IFN-λ2-treated (sensitivity limit: 0,1pg/mg of proteins). Boxes represent median (interquartile range). Data are representative of two independent experiments. a,b, f and g: n=5 per group. c, d and h: n=3 per group. n.s.: not significant. *: $p<0.05$ **: $p<0.001$.

Figure 5: IFN-λ neutralization does not significantly impair IL-22 protective action during pneumonia.

[a] IL-1β concentration assessment by ELISA in BALF. a: n=6 per group. [b] Lung histological analysis from PAO1 infected 24h vehicle treated (upper left panel) or treated with rIL-22 (upper right panel), anti-IFN-λ2 (lower left) or in combination (lower right panel). Magnification x20. Bar = 100µm. b: n=3 per group. Boxes represent median (interquartile range). Data are representative of two independent experiments. *:p<0,05, **: p<0,01, ***: p<0,001.

Andreakos, E., Zanoni, I., Galani, I.E., 2018. Lambda interferons come to light: dual function cytokines mediating antiviral immunity and damage control. Curr. Opin. Immunol. 56, 67–75. doi:10.1016/j.coi.2018.10.007

Aujla, S.J., Chan, Y.R., Zheng, M., Fei, M., Askew, D.J., Pociask, D.A., Reinhart, T.A., McAllister, F., Edeal, J., Gaus, K., Husain, S., Kreindler, J.L., Dubin, P.J., Pilewski, J.M., Myerburg, M.M., Mason, C.A., Iwakura, Y., Kolls, J.K., 2008. IL-22 mediates mucosal host defense against Gram-negative bacterial pneumonia. Nature Medicine 14, 275–281. doi:10.1038/nm1710

Blazek, K., Eames, H.L., Weiss, M., Byrne, A.J., Perocheau, D., Pease, J.E., Doyle, S., McCann, F., Williams, R.O., Udalova, I.A., 2015. IFN-λ resolves inflammation via suppression of neutrophil infiltration and IL-1β production. J. Exp. Med. 212, 845–853. doi:10.1084/jem.20140995

Broquet, A., Jacqueline, C., Davieau, M., Besbes, A., Roquilly, A., Martin, J., Caillon, J., Dumoutier, L., Renauld, J.-C., Heslan, M., Josien, R., Asehnoune, K., 2017. Interleukin-22 level is negatively correlated with neutrophil recruitment in the lungs in a Pseudomonas aeruginosa pneumonia model. Sci Rep 7, 11010. doi:10.1038/s41598-017-11518-0

Cohen, T.S., Prince, A.S., 2013a. Bacterial pathogens activate a common inflammatory pathway through IFNλ regulation of PDCD4. PLoS Pathog. 9, e1003682. doi:10.1371/journal.ppat.1003682

Cohen, T.S., Prince, A.S., 2013b. Activation of inflammasome signaling mediates pathology of acute P. aeruginosa pneumonia. J. Clin. Invest. 123, 1630–1637. doi:10.1172/JCI66142

Egli, A., Santer, D.M., O'Shea, D., Tyrrell, D.L., Houghton, M., 2014. The impact of the interferon-lambda family on the innate and adaptive immune response to viral infections. Emerg Microbes Infect 3, e51. doi:10.1038/emi.2014.51

Eidenschenk, C., Rutz, S., Liesenfeld, O., Ouyang, W., 2014. Role of IL-22 in microbial host defense. Curr. Top. Microbiol. Immunol. 380, 213–236. doi:10.1007/978-3-662-43492-5_10

Fehrenbach, H., 2001. Alveolar epithelial type II cell: defender of the alveolus revisited. Respir. Res. 2, 33–46. doi:10.1186/rr36

Galani, I.E., Triantafyllia, V., Eleminiadou, E.-E., Koltsida, O., Stavropoulos, A., Manioudaki, M., Thanos, D., Doyle, S.E., Kotenko, S.V., Thanopoulou, K., Andreakos, E., 2017. Interferon-λ Mediates Non-redundant Front-Line Antiviral Protection against Influenza Virus Infection without Compromising Host Fitness. Immunity 46, 875–890.e6. doi:10.1016/j.immuni.2017.04.025

Gallagher, G., Megjugorac, N.J., Yu, R.Y., Eskdale, J., Gallagher, G.E., Siegel, R., Tollar, E., 2010. The Lambda Interferons: Guardians of the Immune–Epithelial Interface and the T-helper 2 Response. https://home.liebertpub.com/jir. doi:10.1089/jir.2010.0081

Guillon, A., Brea, D., Morello, E., Tang, A., Jouan, Y., Ramphal, R., Korkmaz, B., Perez-Cruz, M., Trottein, F., O'Callaghan, R.J., Gosset, P., Si-Tahar, M., 2016. Pseudomonas aeruginosa proteolytically alters the interleukin 22-dependent lung mucosal defense. Virulence 8, 1–11. doi:10.1080/21505594.2016.1253658

Hernández, P.P., Mahlakõiv, T., Yang, I., Schwierzeck, V., Nguyen, N., Guendel, F., Gronke, K., Ryffel, B., Hölscher, C., Dumoutier, L., Renauld, J.-C., Suerbaum, S., Staeheli, P., Diefenbach, A., 2015. Interferon-λ and interleukin 22 act synergistically for the induction of interferon-stimulated genes and control of rotavirus infection. Nat. Immunol. 16, 698–707. doi:10.1038/ni.3180

Kollef, M.H., Chastre, J., Fagon, J.-Y., François, B., Niederman, M.S., Rello, J., Torres, A., Vincent, J.-L., Wunderink, R.G., Go, K.W., Rehm, C., 2014. Global Prospective Epidemiologic and Surveillance Study of Ventilator-Associated Pneumonia due to Pseudomonas aeruginosa*. Crit. Care Med. 42, 2178. doi:10.1097/CCM.0000000000000510

Koltsida, O., Hausding, M., Stavropoulos, A., Koch, S., Tzelepis, G., Ubel, C., Kotenko, S.V., Sideras, P., Lehr, H.A., Tepe, M., Klucher, K.M., Doyle, S.E., Neurath, M.F., Finotto, S., Andreakos, E., 2011. IL-28A (IFN-λ2) modulates lung DC function to promote Th1 immune skewing and suppress allergic airway disease. EMBO Mol Med 3, 348–361. doi:10.1002/emmm.201100142

Kotenko, S.V., Gallagher, G., Baurin, V.V., Lewis-Antes, A., Shen, M., Shah, N.K., Langer, J.A., Sheikh, F., Dickensheets, H., Donnelly, R.P., 2003. IFN-lambdas mediate antiviral protection through a distinct class II cytokine receptor complex. Nat. Immunol. 4, 69–77. doi:10.1038/ni875

Lazear, H.M., Nice, T.J., Diamond, M.S., 2015. Interferon-λ: Immune Functions at Barrier Surfaces

and Beyond. Immunity 43, 15–28. doi:10.1016/j.immuni.2015.07.001
Lebreton, A., Lakisic, G., Job, V., Fritsch, L., Tham, T.N., Camejo, A., Matteï, P.-J., Regnault, B., Nahori, M.-A., Cabanes, D., Gautreau, A., Ait-Si-Ali, S., Dessen, A., Cossart, P., Bierne, H., 2011. A bacterial protein targets the BAHD1 chromatin complex to stimulate type III interferon response. Science 331, 1319–1321. doi:10.1126/science.1200120
Leiva-Juárez, M.M., Kolls, J.K., Evans, S.E., 2017. Lung epithelial cells: therapeutically inducible effectors of antimicrobial defense. Mucosal Immunol 102, 245. doi:10.1038/mi.2017.71
Li, A., Gan, Y., Wang, R., Liu, Y., Ma, T., Huang, M., Cui, X., 2015. IL-22 Up-Regulates β-Defensin-2 Expression in Human Alveolar Epithelium via STAT3 but Not NF-κB Signaling Pathway. Inflammation 38, 1191–1200. doi:10.1007/s10753-014-0083-z
Lyczak, J.B., Cannon, C.L., Pier, G.B., 2002. Lung infections associated with cystic fibrosis. Clin. Microbiol. Rev. 15, 194–222. doi:10.1128/CMR.15.2.194-222.2002
Martin, J.C., Wolk, K., Bériou, G., Abidi, A., Witte-Händel, E., Louvet, C., Kokolakis, G., Drujont, L., Dumoutier, L., Renauld, J.-C., Sabat, R., Josien, R., 2017. Limited Presence of IL-22 Binding Protein, a Natural IL-22 Inhibitor, Strengthens Psoriatic Skin Inflammation. J. Immunol. 198, 3671–3678. doi:10.4049/jimmunol.1700021
Moyat, M., Bouzourene, H., Ouyang, W., Iovanna, J., Renauld, J.C., Velin, D., 2017. IL-22-induced antimicrobial peptides are key determinants of mucosal vaccine-induced protection against H. pylori in mice. Mucosal Immunol 10, 271–281. doi:10.1038/mi.2016.38
Odendall, C., Voak, A.A., Kagan, J.C., 2017. Type III IFNs Are Commonly Induced by Bacteria-Sensing TLRs and Reinforce Epithelial Barriers during Infection. J. Immunol. 199, 3270–3279. doi:10.4049/jimmunol.1700250
Pekarek, V., Srinivas, S., Eskdale, J., Gallagher, G., 2007. Interferon lambda-1 (IFN-λ1/IL-29) induces ELR[−] CXC chemokine mRNA in human peripheral blood mononuclear cells, in an IFN-γ-independent manner. Genes and Immunity 2007 8:2 8, 177. doi:10.1038/sj.gene.6364372
Planet, P.J., Parker, D., Cohen, T.S., Smith, H., Leon, J.D., Ryan, C., Hammer, T.J., Fierer, N., Chen, E.I., Prince, A.S., 2016. Lambda Interferon Restructures the Nasal Microbiome and Increases Susceptibility to Staphylococcus aureus Superinfection. MBio 7, e01939–15. doi:10.1128/mBio.01939-15
Sabat, R., Ouyang, W., Wolk, K., 2013. Therapeutic opportunities of the IL-22–IL-22R1 system. Nat Rev Drug Discov 13, 21–38. doi:10.1038/nrd4176
Sheppard, P., Kindsvogel, W., Xu, W., Henderson, K., Schlutsmeyer, S., Whitmore, T.E., Kuestner, R., Garrigues, U., Birks, C., Roraback, J., Ostrander, C., Dong, D., Shin, J., Presnell, S., Fox, B., Haldeman, B., Cooper, E., Taft, D., Gilbert, T., Grant, F.J., Tackett, M., Krivan, W., McKnight, G., Clegg, C., Foster, D., Klucher, K.M., 2003. IL-28, IL-29 and their class II cytokine receptor IL-28R. Nat. Immunol. 4, 63–68. doi:10.1038/ni873
Sommereyns, C., Paul, S., Staeheli, P., Michiels, T., 2008. IFN-lambda (IFN-lambda) is expressed in a tissue-dependent fashion and primarily acts on epithelial cells in vivo. PLoS Pathog. 4, e1000017. doi:10.1371/journal.ppat.1000017
Syedbasha, M., Egli, A., 2017. Interferon Lambda: Modulating Immunity in Infectious Diseases. Front Immunol 8, 119. doi:10.3389/fimmu.2017.00119
Thorley, A.J., Grandolfo, D., Lim, E., Goldstraw, P., Young, A., Tetley, T.D., 2011. Innate immune responses to bacterial ligands in the peripheral human lung--role of alveolar epithelial TLR expression and signalling. PLoS ONE 6, e21827. doi:10.1371/journal.pone.0021827
Trevejo-Nunez, G., Elsegeiny, W., Conboy, P., Chen, K., Kolls, J.K., 2016. Critical Role of IL-22/IL22-RA1 Signaling in Pneumococcal Pneumonia. J. Immunol. 197, 1877–1883. doi:10.4049/jimmunol.1600528
Whittington, H.A., Armstrong, L., Uppington, K.M., Millar, A.B., 2004. Interleukin-22: a potential immunomodulatory molecule in the lung. Am. J. Respir. Cell Mol. Biol. 31, 220–226. doi:10.1165/rcmb.2003-0285OC
Witte, E., Witte, K., Warszawska, K., Sabat, R., Wolk, K., 2010. Interleukin-22: a cytokine produced by T, NK and NKT cell subsets, with importance in the innate immune defense and tissue protection. Cytokine Growth Factor Rev. 21, 365–379. doi:10.1016/j.cytogfr.2010.08.002
Wolk, K., Kunz, S., Asadullah, K., Sabat, R., 2002. Cutting edge: immune cells as sources and targets

of the IL-10 family members? J. Immunol. 168, 5397–5402. doi:10.4049/jimmunol.168.11.5397
Wolk, K., Witte, E., Wallace, E., Döcke, W.-D., Kunz, S., Asadullah, K., Volk, H.-D., Sterry, W., Sabat, R., 2006. IL-22 regulates the expression of genes responsible for antimicrobial defense, cellular differentiation, and mobility in keratinocytes: a potential role in psoriasis. Eur. J. Immunol. 36, 1309–1323. doi:10.1002/eji.200535503
Wolk, K., Witte, K., Witte, E., Proesch, S., Schulze-Tanzil, G., Nasilowska, K., Thilo, J., Asadullah, K., Sterry, W., Volk, H.-D., Sabat, R., 2008. Maturing dendritic cells are an important source of IL-29 and IL-20 that may cooperatively increase the innate immunity of keratinocytes. J Leukoc Biol 83, 1181–1193. doi:10.1189/jlb.0807525
Xue, M., Zhao, J., Ying, L., Fu, F., Li, L., Ma, Y., Shi, H., Zhang, J., Feng, L., Liu, P., 2017. IL-22 suppresses the infection of porcine enteric coronaviruses and rotavirus by activating STAT3 signal pathway. Antiviral Res. 142, 68–75. doi:10.1016/j.antiviral.2017.03.006
Yan, B., Chen, F., Xu, L., Wang, Y., Wang, X., 2017. Interleukin-28B dampens airway inflammation through up-regulation of natural killer cell-derived IFN-γ. Sci Rep 7, 3556. doi:10.1038/s41598-017-03856-w
Ye, L., Schnepf, D., Staeheli, P., 2019. Interferon-λ orchestrates innate and adaptive mucosal immune responses. Nat. Rev. Immunol. 4, 69. doi:10.1038/s41577-019-0182-z
Zenewicz, L.A., Flavell, R.A., 2011. Recent advances in IL-22 biology. Int. Immunol. 23, 159–163. doi:10.1093/intimm/dxr001
Zheng, Y., Danilenko, D.M., Valdez, P., Kasman, I., Eastham-Anderson, J., Wu, J., Ouyang, W., 2007. Interleukin-22, a T(H)17 cytokine, mediates IL-23-induced dermal inflammation and acanthosis. Nature 445, 648–651. doi:10.1038/nature05505

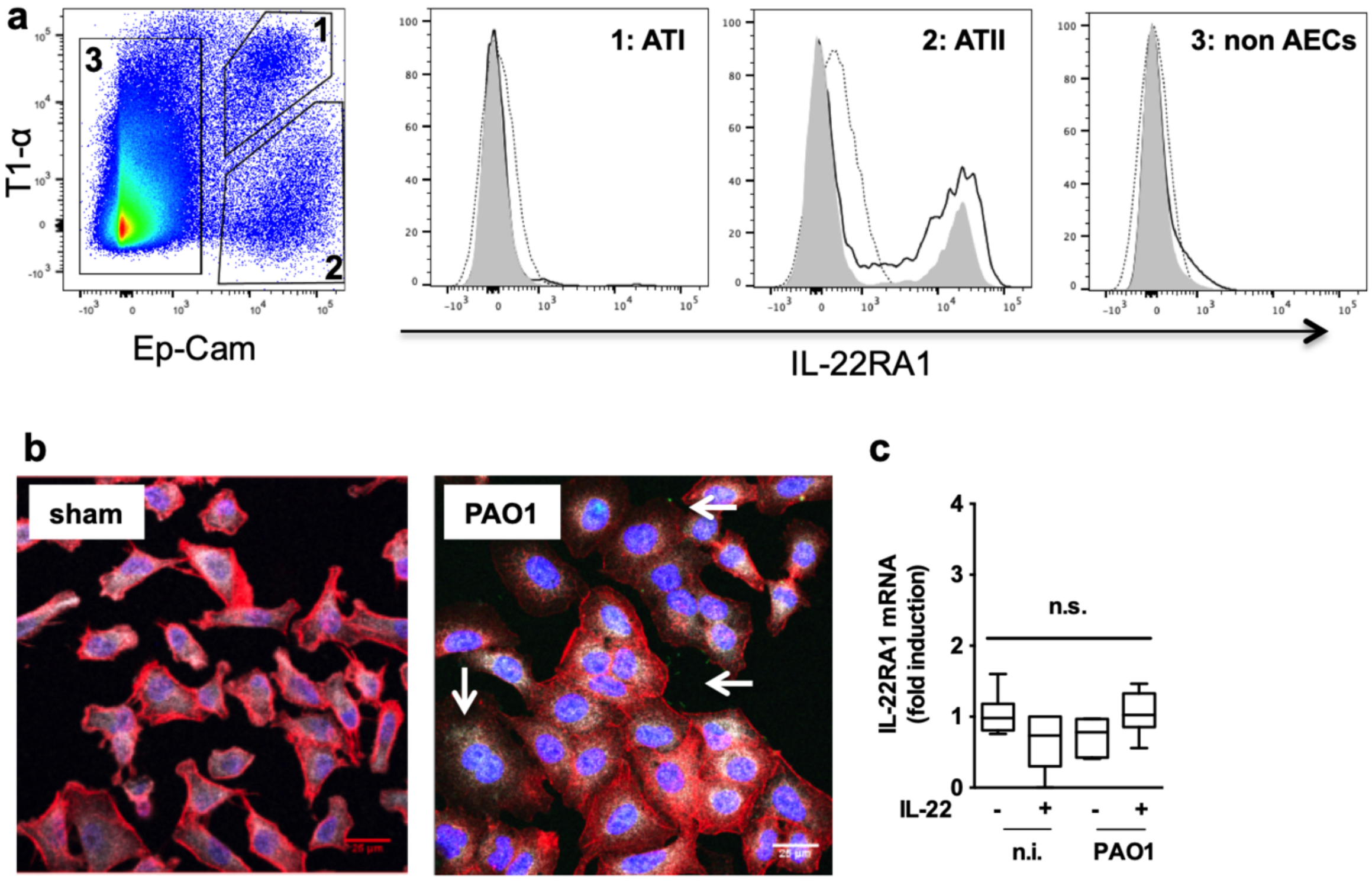

Figure 1: IL-22 signaling is not altered during PAO1 infection in type-II AECs.

[a] IL-22RA1 expression on single $CD45_{neg}$ $CD31_{neg}$ lived cells in the lungs by flow cytometry. ATI: Type-I Alveolar epithelial cells gated as Ep-Cam_{pos} T1-α_{pos}. ATII: Type-II Alveolar epithelial cells gated Ep-Cam_{pos} T1-α_{neg}. Non AECs gated Ep-Cam_{neg}. Dashed line: isotype control Ab. Solid line: IL-22RA1 Ab in sham mice. Filled histogram: IL-22RA1 in infected mice. [b] Confocal microscopy of non-infected (upper panel) and 4h PAO1-infected A549 cells (lower panel). Blue: nuclei, red: β-actin, white: IL-22RA1, green: PAO1-GFP (arrow). Magnification x40. Bar = 25μm. [c] IL-22RA1 mRNA expression by real-time PCR from PAO1-infected A549 cells treated or not with IL-22. Boxes represent median (interquartile range). n.s.: not significant.

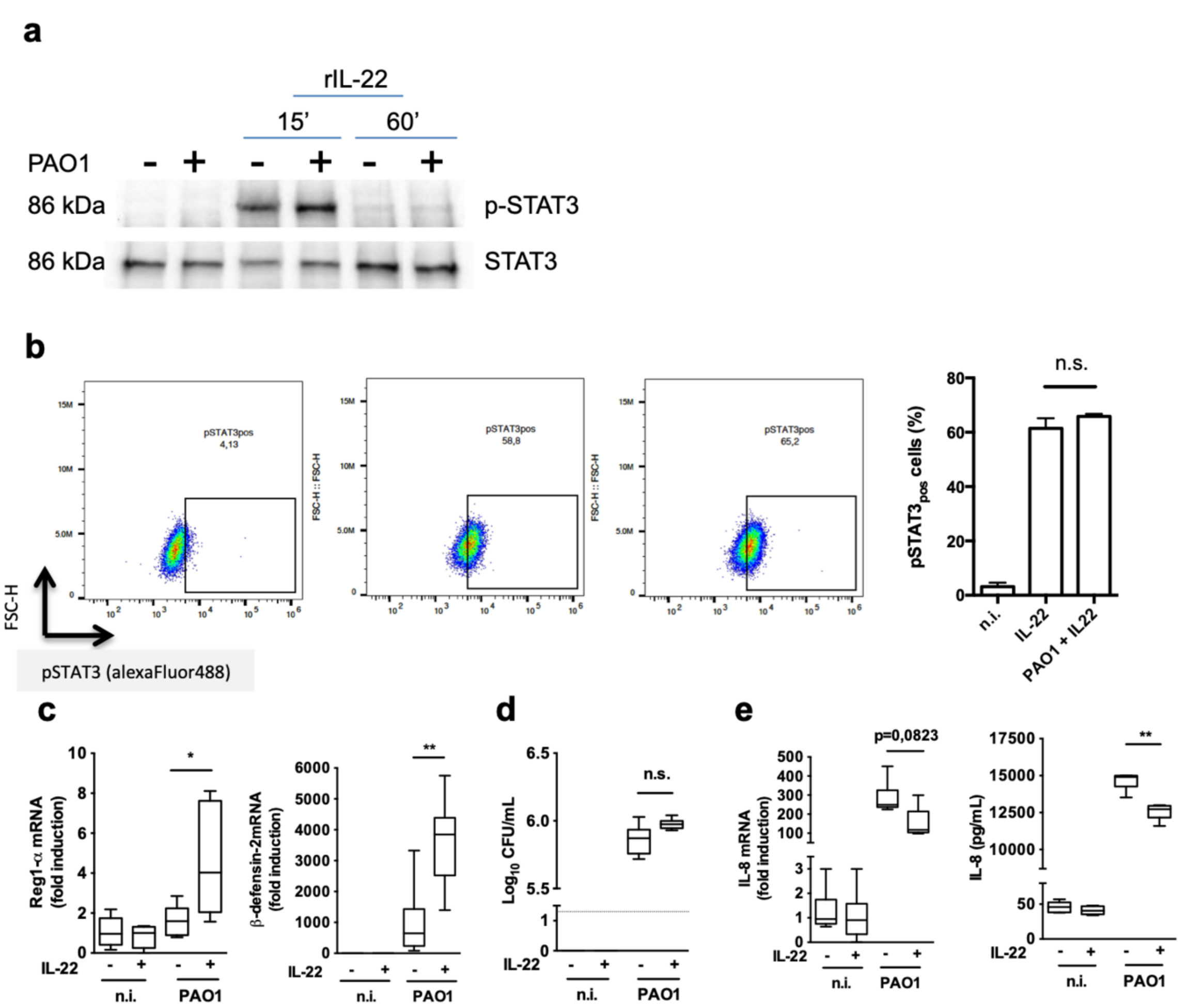

Figure 2: IL-22 incubation modulates cell response to infection

[a] Western blot of phospho-STAT3 expression from non-infected and PAO1-infected A549 cells treated or not with IL-22. [b] p-STAT3 evaluation in 15 minutes infected-A549 by flow cytometry. Dot plots: left: non infected; middle: IL-22 alone; right: IL-22 + PAO1. Right histogram: Percent of A549 expressing p-STAT3 following treatment [c] Reg1-α and β-defensin-2 mRNA expression by real-time PCR from 2h PAO1-infected A549 cells treated or not with IL22. Boxes represent median (interquartile range). [d] Bacterial load in supernatant from 24h PAO1-infected A549 cells treated or not with IL-22. Boxes represent median (interquartile range). Dashed bar: detection threshold [e] IL-8 mRNA relative expression from 2h PAO1-infected A549 cells treated or not with IL-22 (left panel) and IL-8 protein levels by ELISA from 24h PAO1-infected A549 cells treated or not with IL-22 (right panel. sensitivity limit: 2pg/mL). Boxes represent median (interquartile range). Data are representative of two independent experiments. *: $p<0.05$ **: $p<0.001$.

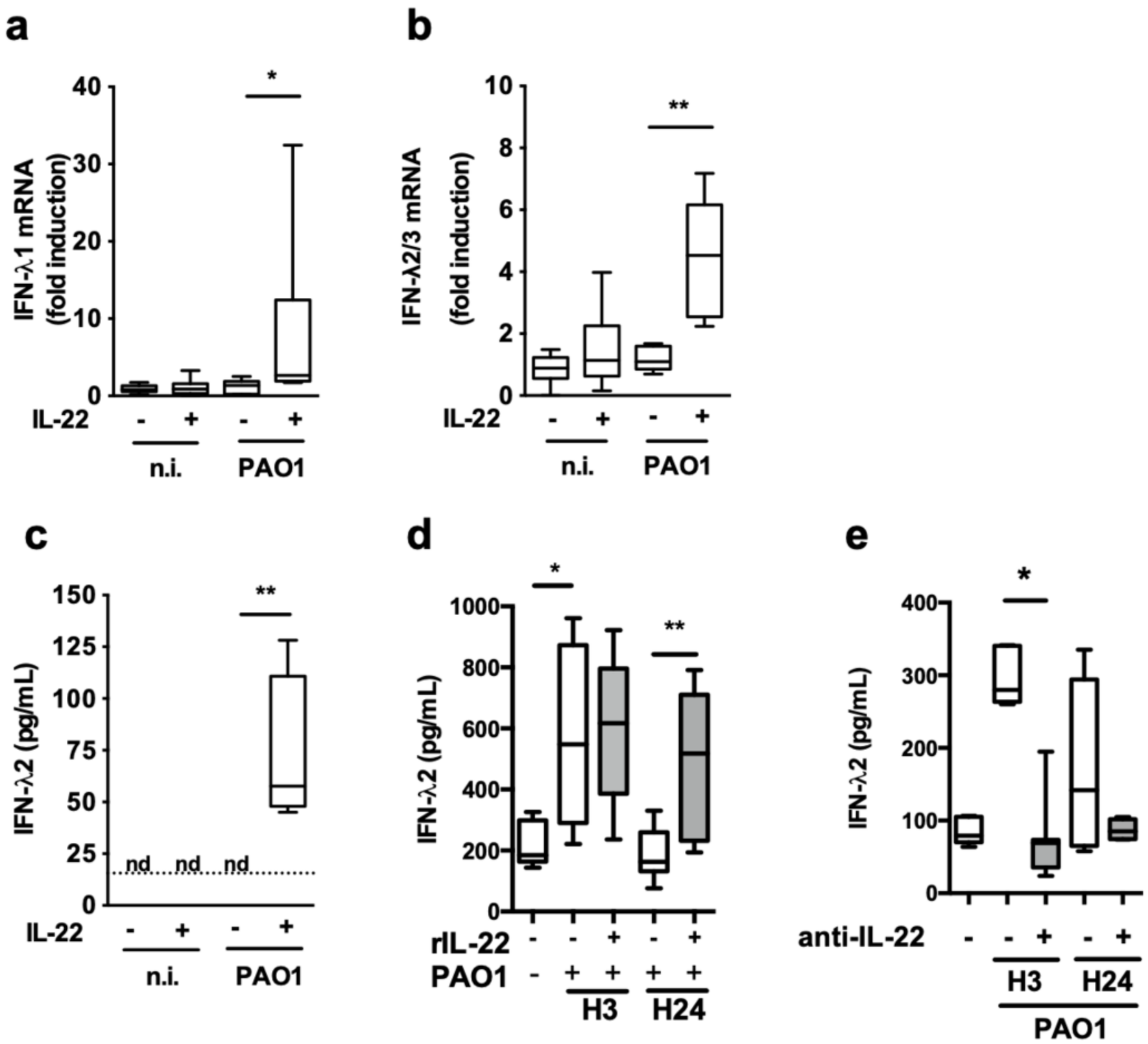

Figure 3: IL-22 enhanced IFN-λ expression in PAO1 infected cells

[a-b] IFN-λ1 and IFN-λ2/3 mRNA relative expression from 2h PAO1-infected A549 cells treated or not with IL-22. Boxes represent median (interquartile range). [c] IFN-λ2 protein levels from 24h PAO1-infected A549 cells treated or not with IL-22 (dashed line: sensitivity limit 15,6pg/mL). Boxes represent median (interquartile range). n.d. : not detected. Data are representatives of two independent experiments. [d] IFN-λ2 quantification by ELISA in BALF of infected mice treated or not with IL-22. n=5 per group. [e] IFN-λ2 quantification by ELISA in BALF of infected mice treated or not with neutralizing anti-IL-22 antibody. n= 4-5 per group Boxes represent median (interquartile range)*: $p<0.05$ **: $p<0.001$

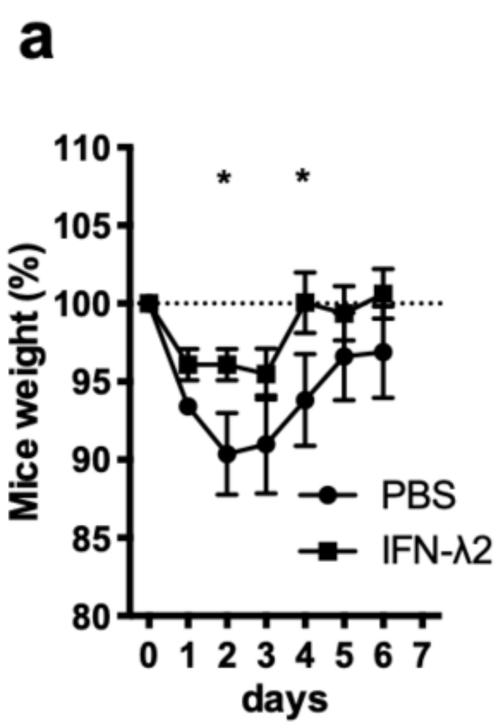

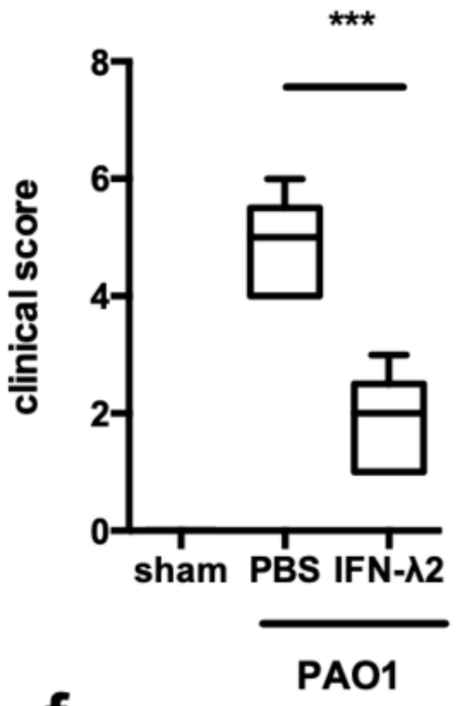

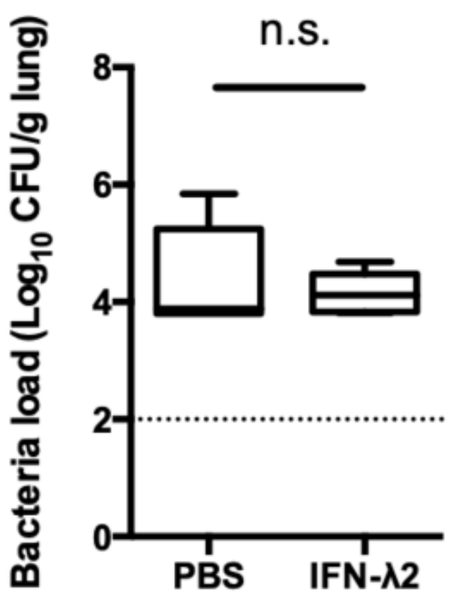

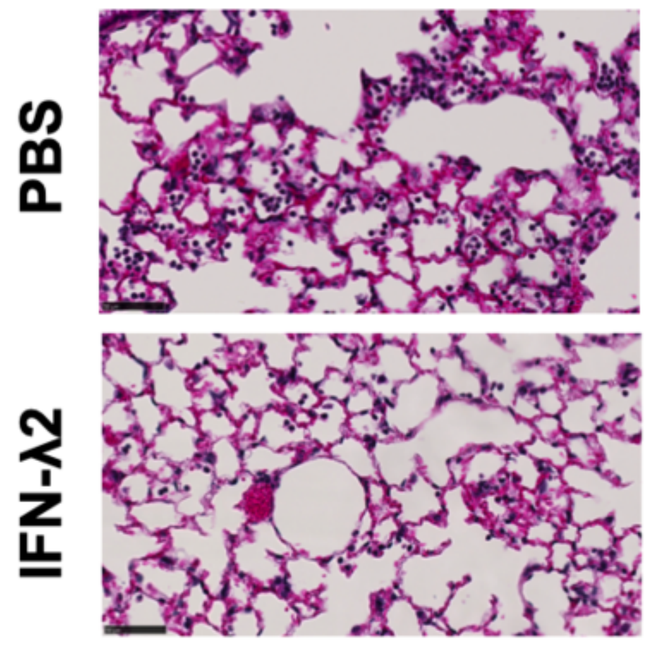

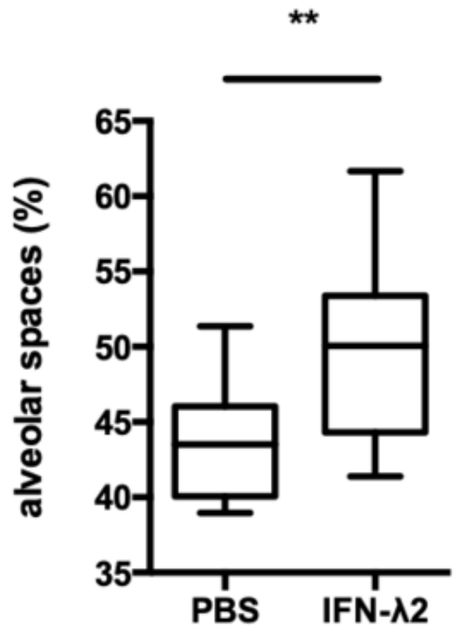

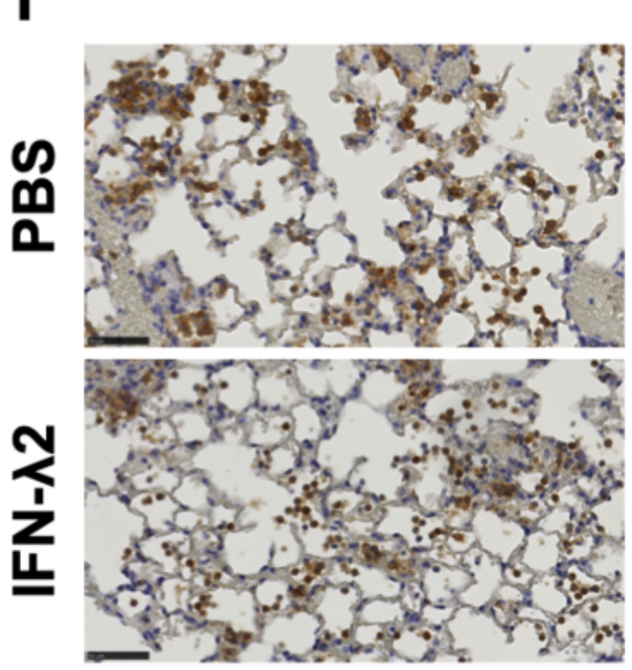

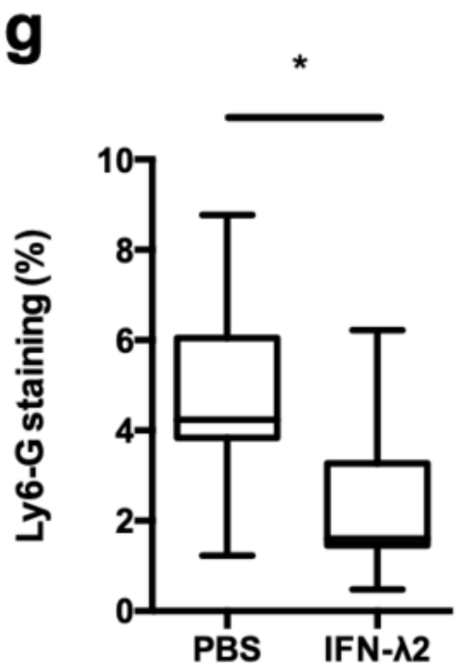

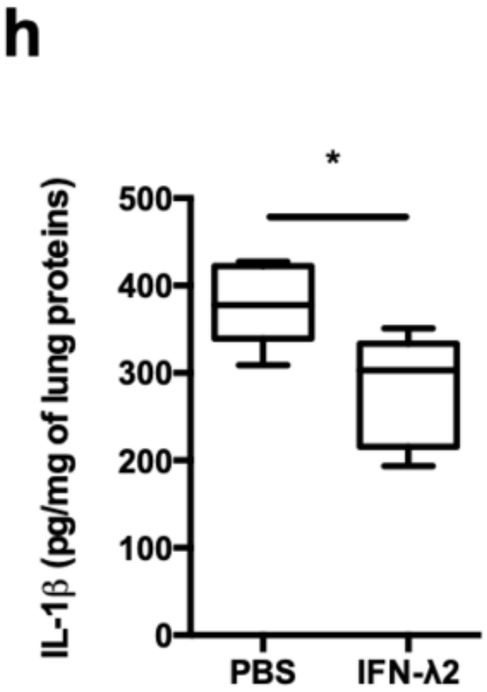

Figure 4: In vivo IFN-λ2 administration improves mice outcome and dampens neutrophil recruitment during infection.

[a] Daily body weight evaluation of infected mice vehicle- or IFN-λ2-treated. [b] Mouse clinical score of 24h-infected mice vehicle- or IFN-λ2-treated. [c] Bacterial counts (expressed in log_{10} colony-forming units (CFU)/gram of organ) in the lungs of 24h-infected mice vehicle-treated or IFN-λ2-treated. Data are representative of two independent experiments. Dashed line: threshold limit [d – left panel] Lung histological analysis from PAO1 infected mice 24h vehicle-treated (upper panel) or IFN-λ2-treated (lower panel). Magnification x40. Bar = 25μm. [d – right panel]. [e] Alveolar space quantification by SIOX analysis of histology slides presented in d (3 mice per group. 4 fields per slide). [f] Ly6-G IHC of lung section from 24h-infected PAO1 mice vehicle-treated (upper panel) or IFN-λ2-treated (lower panel). Magnification x40. Bar = 25μm. [g] Quantification of Ly6-G positive pixels surface area by SIOX analysis of the slides presented in f. (3 mice per group. 4 fields per slide). [h] IL-1β concentration assessment by ELISA in lung homogenates of 24h infected mice vehicle-treated or IFN-λ2-treated (sensitivity limit: 0,1pg/mg of proteins). Boxes represent median (interquartile range). Data are representative of two independent experiments. a,b, f and g: n=5 per group. c, d and h: n=3 per group. n.s.: not significant. *: $p<0.05$ **: $p<0.001$.

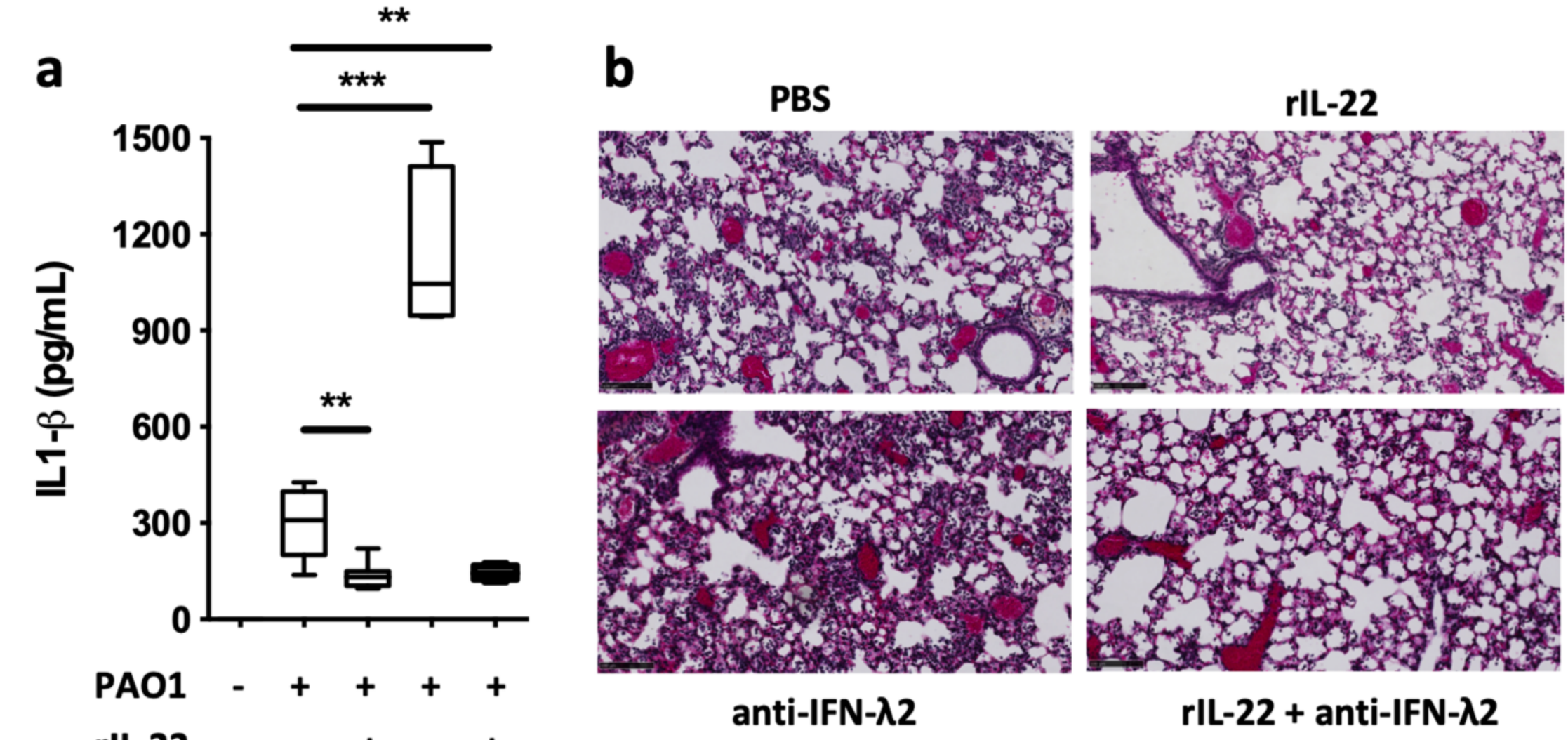

Figure 5: IFN-λ neutralization does not significantly impair IL-22 protective action during pneumonia.

[a] IL-1β concentration assessment by ELISA in BALF. a: n=6 per group. [b] Lung histological analysis from PAO1 infected 24h vehicle treated (upper left panel) or treated with rIL-22 (upper right panel), anti-IFN-λ2 (lower left) or in combination (lower right panel). Magnification x20. Bar = 100µm. b: n=3 per group. Boxes represent median (interquartile range). Data are representative of two independent experiments. *:p<0,05, **: p<0,01, ***: p<0,001.

Table 1: Sequences of primers used for RT-PCR.

Primers		Sequences	Size
β-actin	Forward	5'CCCAGCCATGTACGTTGTA'3	126pb
	Reverse	5'AGGGCATACCCCTCGTAGATG'3	
IL-22RA1	Forward	5'CTGACACAGAGTTCCTTGG'3	406pb
	Reverse	5'CCTAAGTAGGTGATCTCGG'3	
BD-2	Forward	5'GCCATGAGGGTCTTGTATCTC'3	236pb
	Reverse	5'TCTGAATCCGCATCAGCCAC'3	
REG1α	Forward	5'TGGAAGGATGTGCCTTGTGAAGACA'3	178pb
	Reverse	5'AGGCAAACTCAGCAGAGAAGAGAGT'3	
IL-8	Forward	5'CTGGCCGTGGCTCTCTTGG'3	185pb
	Reverse	5'ATTTCTGTGTTGGCGCAGTGTG'3	
IFN-λ2/3	Forward	5'GACATGACCGGGGACTGCATG'3	589pb
	Reverse	5'GACACACAGGTCCCCGCTGG'3	
IFN-λ1	Forward	5'GCCATGGCTGCAGCTTGGAC'3	602pb
	Reverse	5'GGTGGACTCAGGGTGGGTTGAC'3	